Optics and Lasers in Engineering 169 (2023) 107724

Contents lists available at ScienceDirect

Optics and Lasers in Engineering

journal homepage: www.elsevier.com/locate/optlaseng

Beam shaping with a deformable mirror for gap bridging in autogenous laser butt welding

Yongcui Mi [a], Pasquale Guglielmi [b,*], Morgan Nilsen [a], Fredrik Sikström [a], Gianfranco Palumbo [b], Antonio Ancona [a,c]

[a] Department of Engineering Science, University West, 461 86 Trollhättan, Sweden
[b] Department of Mechanics, Mathematics and Management, Politecnico di Bari, via Orabona 4, 70125 Bari, Italy
[c] Physics Department, University of Bari "Aldo Moro", via Orabona 4, 70125 Bari, Italy

ARTICLE INFO

Keywords:
Laser beam welding
Beam shaping
Process monitoring
Microstructure
Steel

ABSTRACT

In autogenous laser butt welding the variability of the joint gap can cause problems in terms of weld seam quality. A suitable strategy to alleviate this is to dynamically shape the laser beam instead of a circular-shaped beam with typical Gaussian or top hat distributions. Currently available systems cannot reach sufficient performance due to both the real time control system for the shape variation and the limited laser power currently manageable. In the present work, the possibility of bridging the joint gap during welding using a deformable mirror to elongate the focused laser beam from circular to transversal elliptical shape was investigated. The effect of the beam shaping on the geometry of the weld pool and of the weld cross sections was analysed, for different values of the gap in comparison with a circular Gaussian beam. It was demonstrated that the adoption of a transversal elliptical laser beam makes the welding process more stable, especially for large gaps (i.e. larger than the circular beam radius). Thanks to the beam shaping, the extension of the fused zone (in terms of the cross section area, height and width) resulted to be less sensitive to the gap's dimension; in addition, the extension of the heat affected zone and the presence of undercuts were evidently reduced.

1. Introduction

The demand to increase productivity and robustness of laser beam welding (LBW) motivates the industry to progress this technology beyond current state of the art of automation and control. An emerging possibility is the introduction of laser beam (LB) shaping in autogenous butt welding. Autogenous LBW is characterized by a spatially concentrated and low heat input enabling narrow seams at high welding travel speeds and with limited residual stresses and distortions. To benefit from this, in square joints butt welding it is necessary to have sufficient consistency of the parts to be joined, which implies tight tolerances for the joint fit, sufficient alignment and that the thermal distortion during welding is limited [1]. It is usually possible to reach necessary requirements through joint preparation and clamping devices, but these actions come with a cost that increases with the tightness of the required tolerances.

Usually, in autogenous LBW the beam power density distribution in focus is fixed (typically circular Gaussian or top hat) and the joint gap width that can be tolerated is of the order of the focused effective LB diameter. The beam simply passes through if the gap is too large. As a rule of thumb, the gap width should be less than 10% of the thickness of the thinnest workpiece member [2]. It could also be mentioned that it is usually difficult to start welding in an area with a large gap compared to maintaining welding through a short section of larger gap, where it is sometimes possible to continue bridging.

The traditional way of alleviating the problem of joint gap variations and/or too large a gap is to apply filler wire. However, the addition of filler metal requires the proper access to the joining zone both with the filler wire and the LB. Most arrangements using filler wire in LBW is direction dependent which in turn imposes restrictions in the robotic manipulation. Another drawback is that the use of wire filler metal requires additional hardware, i.e., a wire feeder and filler, that both add costs. Finally, wire feed welding is typically slower which leads to a longer cycle time. An appealing alternative to wire feed welding to alleviate joint gap variations is to use LB shaping which consists in tailoring the power density distribution to distribute the heat input in such a way as to promote gap bridging. Most of the currently available beam shaping devices are still limited as either it is not possible to change the beam shape on-the-fly or the optical power they can handle is limited.

Diffractive optical elements (DOEs) are widely used tools for beam shaping. Hansen et al. [3] welded multiple sheets with butt joint configuration in a single pass using a DOE beam shaping unit. The beam

* Corresponding author.
E-mail address: pasquale.guglielmi@poliba.it (P. Guglielmi).

https://doi.org/10.1016/j.optlaseng.2023.107724
Received 2 March 2023; Received in revised form 9 May 2023; Accepted 28 June 2023

was shaped into multiple spots and aligned in a row perpendicular to the welding direction. Results showed that the welds were widened by using multiple spots, which enhanced the gap bridgability. Similarly, Volpp [4] divided the beam in up to four separate spots arranged in a raw or in a 2×2 matrix with different splitting of the total power among the spots. Gap bridgability was evaluated by conducting experiments on samples with opening gaps. High speed imaging was used to evaluate the amount of spatters. Each spot produced a different keyhole and, by dividing symmetrically the keyholes with respect to the gap and with adequate separation, a better gap bridgability was demonstrated compared to a single spot. This was ascribed to the effect of the beam shaping on the melt flow. The high-intensity spots created keyholes next to each other that pushed the melt towards the center of the gap. At the same time, additional low-intensity spots enabled to reduce spattering by stabilizing the weld pool dynamics. Kristiansen et al. [5] used the same approach, based on a diffractive optical element which split the LB into a 9-spot pattern, to weld four sheets in butt joint configuration. Although the weld quality was satisfactory, nonetheless severe porosities were observed in some welds. Rasch et al. [6] used DOEs to create different beam shapes, i.e., a ring, a line and a row of spots, for investigating their influence on conduction mode welding of aluminum–copper alloys. They found that beam shaping can improve stability and enlarge the weld seam cross section in comparison to a defocussed multimode spot of the same size. In addition, a better seam surface roughness was achieved. DOEs have been used also to shape the beam not only in a plane orthogonal to it propagation direction but also along its propagation axis by creating multiple beam waists. This was used to provide a more homogeneous heat input inside the keyhole to avoid collapses, stabilize the welding and reduce spatters [7]. However, this beam shaping solution might not be relevant for gap bridging. Unfortunately, DOEs need to be carefully designed in advance according to the characteristics of the laser source and the desired beam shape to be produced in the focal plane. For instance, it is necessary to define the number of spots, their separation and spatial arrangement and power splitting depending on the workpiece thickness and gap width to be bridged. This is not always possible since workpiece thickness, weld geometry, misalignments and gap width have variations in industrial manufacturing. In addition, in most practical cases welding direction is not always straight along the workpiece. Therefore, any change of the welding direction will change the arrangements of the multiple spots and their power distribution with respect to the travel front and, thus, the melt flow behavior.

Another possibility that has been widely explored is to quickly oscillate the beam along predefined paths during welding. Galvoscanners can be used for fast “writing” of an intensity profile in LBW applications [8–12]. Two- and three-dimensional scanning pattern with oscillation frequency up to 10 kHz [13] can be produced. Meng et al. [8] welded aluminum/steel dissimilar metals in a butt joint configuration using hybrid arc-laser with LB oscillated by a galvoscanner. The macro- and micrographic images of the welds showed even weld seam surfaces and a uniform interface between the dissimilar metals. The tensile properties and the bending properties were also enhanced. Chen et al. [9] used motorized mirror (YW52 Precitec GmbH, Germany) to oscillate the LB during welding of titanium/aluminum dissimilar materials in butt joint configuration. The microstructure and tensile properties were evaluated, and their results showed that, with proper oscillating frequency and amplitude, the weld seam had excellent intermetallic compounds distribution and mechanical properties. In [14], the authors used a galvoscanner to shape the LB during overlap welding of aluminum alloys with partial penetration. Interface width, penetration and interface defects were evaluated in different beam shaping conditions. The conclusion was that by shaping the beam over 10 kHz desired weld width and penetration depth could be achieved, the process window was enlarged giving less defects and stable seam geometry. Dittrich et al. [15] used a galvoscanner to oscillate the beam during autogenous butt welding of hot crack sensitive aluminium alloys. The LB rotation along a circular path allowed suppression of hot cracks in the weld metal thanks to the change of the temperature gradient, although some cracks occurred in the heat affected zone (HAZ). The main drawback of beam oscillation is that state-of-the-art scanners are still too slow for high-speed LBW. In addition, during beam oscillation, hot spots may be formed in the intensity distribution of the heat inputs at the points of the paths where the beam changes abruptly direction.

Möller et al. [16] utilized a multifocal optics consisting of two wedges to split the incoming LB into four single beams and focused them in one welding zone to weld e-mobility components made of casted and wrought aluminum alloys. Before being split, the pristine LB was coming from a laser source that allowed dividing the laser power between the core and the ring of the delivery fiber, thus varying the power distribution. The combination of these two beams shaping technologies allowed stabilization of the keyhole thanks to the flexibility of such system to adapt the heat source onto the welding zone. In this way, it was possible to get deeper weld penetration, increase the keyhole area and the weld pool extension and, at the same time, reduce spatter formation.

In several other works, a double cladded fiber has been used for beam shaping. Here, two variable power levels are coupled into the core and the inner cladding of the delivery fiber, enabling rapid, on-the-fly tuning of the power density distribution [17,18]. In [17], the authors obtained the LB shape by a double cladded fiber and studied the influence and possibilities of beam shaping on steel/copper dissimilar lap joints with copper on the topside. Weld seam surface appearance and topography, as well as the cross sections of the welds were evaluated. The results showed that by properly adjusting the beam shapes, spattering and pool beam coupling in copper surface could be avoided. In [18] various test results of LBW with beam shaping using the double cladded fiber technology are also presented. The experiments were performed on welding of steel, aluminum, and copper in different applications, including powertrain, components of the car bodies and tubes. Their test results have shown that welding with beam shaping can provide better stability and efficiency. Mohammadpour et al. [19] used an adjustable ring mode fiber laser for bead-on-plate welding and compared results with those obtained with a single mode fiber laser. Three different beam shapes were investigated by concentrating the laser power either in the central part of the fiber or totally in the ring or splitting the power equally among the two waveguiding parts of the fiber. In the first case, deeper penetration was obtained in comparison to single mode fiber laser, while in the second case penetration was shallower but a significant reduction of spatters was observed. It was shown that by dividing the laser power between the center and the ring allowed enlarging the keyhole aperture thus stabilizing it.

A very advanced beam shaping technique recently applied to LBW is coherent beam combining (CBC) through optical phased array (OPA) [14]. It splits a low power LB into several channels, amplifies each channel separately, and recombines them into one high-power beam. Over 10 kW optical power can be controlled dynamically by its 2D position, focus, shape, at MHz frequencies [14,20]. One drawback of this method is that the OPA welding head is bulky, which might limit the flexibility of integrating it in an automatic production line. Nonetheless it was shown that switching between different intensity distributions has noticeable impact on the longitudinal as well as transversal geometry of the keyhole [21], thus promising to be a suitable tool for fast adaptation of the keyhole to varying welding conditions. In this regard, the adoption of double-cladded fiber and coherent beam combining for beam shaping to solve the problem of bridgability in butt joints has been so far scarcely explored.

Deformable mirrors represent a further and very promising technology for beam shaping of high-power continuous wave beams. Such adaptive optics devices, originally developed for astronomical purposes to improve the quality of the images acquired by telescopes by compensating for the aberrations introduced by the atmosphere, have recently found application also in the field of industrial laser cutting [22] Furthermore, new types of deformable mirror dedicated to high-power laser beam shaping have been proposed [23]. Here, a deformable mirror was developed for a high power CO_2 laser source, which enabled to change the pristine Gaussian beam profile into a top-hat energy distribution [23]. However, such mirror required water-cooling and showed some limitations in terms of flexibility to produce different beam shapes. Recently, a deformable mirror system, consisting of piezoelectric actuators directly bonded to a high reflective flexible glass membrane, was shown to enable beam shaping of a multi-kilowatt beam without requiring any active cooling. In principle such system can produce an infinite number of aberrations modes that make it possible to obtain different beam shapes. Beam shaping using a deformable mirror was shown to modify the weld pool geometry and, thus, the joint cross section in conduction mode LBW [24,25]. In [23], the originally circular LB was transformed into an elliptical one with major axis oriented along or transversely to the welding direction. Conduction bead-on-plate welding of Ti64 was conducted with 1kW laser power and the results were compared to circular beam shape with the same power level. It was shown the possibility to tailor melt pool free surface geometry, cross section, microstructure, and hardness profiles by changing the beam shape. Potentially such deformable mirror device can change the laser beam shape at a rate of 100 Hz, which is promising for adaptive control during welding.

In this work, we investigate the possibility of bridging the gap during autogenous LB butt welding by using a shape that elongates the focused LB from circular to elliptical shape with major axis of the ellipse oriented transversely with respect to the welding direction. The influence of such beam shape on the weld pool shape, and weld cross section geometry has been investigated at different gap widths and compared to the case of a reference circular Gaussian beam.

2. Experimental setup and methodology

The welding setup consisted of a water-cooled high-power ytterbium-doped fiber laser, a CNC gantry, fixtures, shielding gas supply equipment, an imaging system, and a deformable mirror system. The methodology includes welding parameters description, joint gap width and weld pool top surface geometry measurement and methods for analyzing the weld seam cross sections.

2.1. The laser beam welding setup

The LBW setup is shown in Fig. 1. The LB, with a wavelength of 1070 nm, was generated by a 6 kW IPG system (mod. YRL-6000-S) and guided to the welding head through a 200 μm core diameter optical fiber. The welding head comprised a f = 76 mm collimator and a f = 400 mm focusing lens. It was manipulated by a CNC gantry from Isel® Germany (mod. M40). To avoid back reflections into the optics the welding head was mounted on to the gantry with an inclination angle of 5° in the travel direction with respect to the workpiece surface normal. Argon was supplied as shielding gas to protect the process to both the top and root side of the workpiece at flow rates of 10 L/min 15 L/min, respectively. Argon was also supplied in front of the focusing lens of the welding head to protect it from spatters. The total laser power used was 2100 W and the welding travel speed was 15 mm/s.

2.2. Camera system

An imaging system was integrated coaxially with the LB in the welding head to capture and measure the weld pool free surface at the workpiece top surface. It consisted of a camera (SP5000M-CX4, from JAI), an imaging lens with f = 150 mm and a hard-coated band pass filter (center wavelength at 450 nm and full width at half max of 10 nm). With this configuration, the acquired images had a size of 512*2048 pixels and the resolution was around u=14 μm/pixel, obtained by calibration of the vision system using a checkerboard with light and dark squares with square size of 1 mm^2. To increase the image contrast, three LEDs (450 nm center wavelength) were mounted with high angle (smaller than 30° with respect to the workpiece surface normal) to illuminate the region of the weld pool. The exposure time was 500 μs and the acquisition frame rate was 200 frames per second.

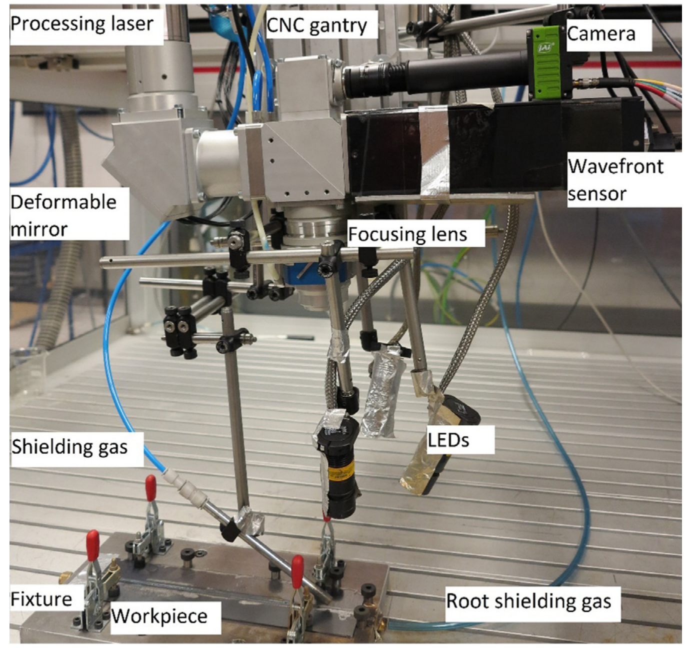

Fig. 1. Welding setup.

2.3. Deformable mirror system

The beam shaping system (from Dynamic Optics S.r.l.) consisted of a deformable mirror, a Shack-Hartmann wavefront sensor and a control unit. The system was directly integrated into the welding head, as shown in Fig. 2. The deformable mirror was installed after the collimator and before the dichroic mirror, at an angle of 45° to the incident beam. It consisted of a thin glass flexible membrane and 19 piezoelectric actua-

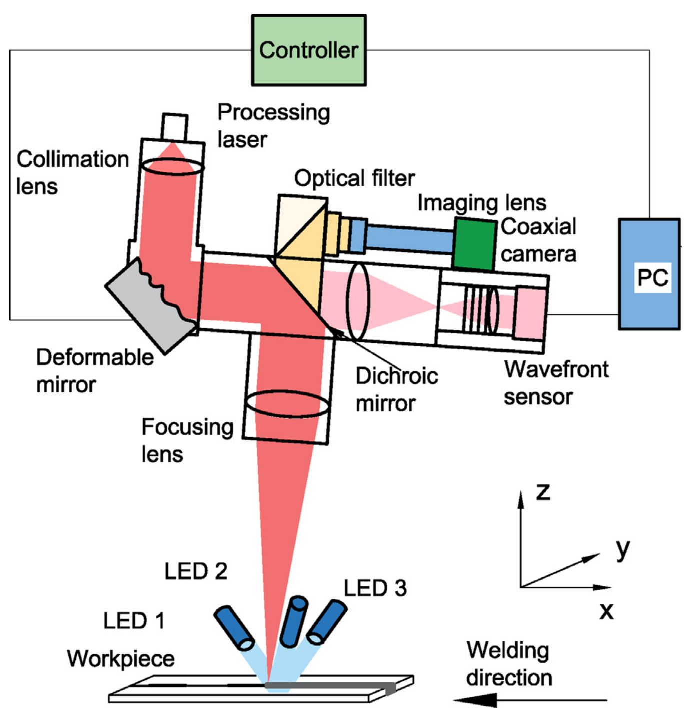

Fig. 2. Schematic of the setup showing the components and their arrangement.

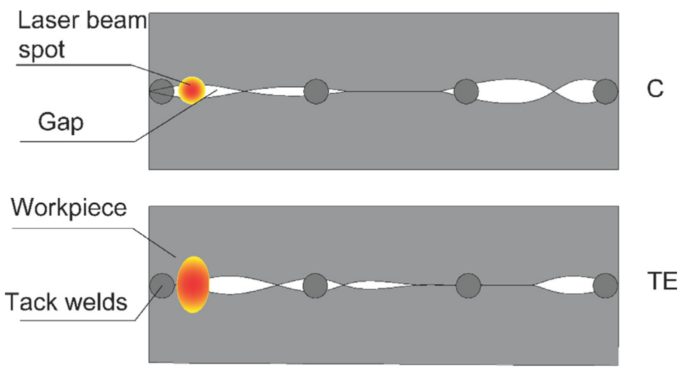

Fig. 3. A schematic diagram of the two welding cases.

tors that were activated to pull and push the membrane to deform its curvature and, in this way, change the wavefront after reflection. The membrane is made of fused silica (thickness: 0.8 mm) is coated with a multi-layer dielectric coating to achieve high reflectivity (R > 99.99) at 1070 nm and low absorptivity ($A < 10^{-5}$). The low absorption of the dielectric coating reduced heating of the mirror even during long exposure at high-power laser levels. Therefore, no water-cooling is needed for the mirror. The laser beam impinged on the deformable mirror with a diameter of around 20 mm and for laser beam with power of 2100 W, the irradiance on the surface of the mirror was around 6.688 W/(mmˆ2). The actuators were disposed in two concentric oval rings to match the incident beam size. The stroke of each actuator was ±5 µm. The wavefront sensor was placed opposite to the deformable mirror and behind the dichroic mirror, so that it captured the light reflected by the deformable mirror and leaking from the dichroic mirror. In this way, it was possible to measure in real time the aberrations introduced in the beam by the deformable mirror according to the positions of the actuators. At each desired beam shape in the LB focal plane, corresponded a combination of aberrations in the beam. Once defined the desired beam shape and thus the wavefront, a feedback control unit enabled to keep that shape by acting in real time on the piezo actuators. In this way, any thermal drift was compensated. A more detailed description of the system can be found in [24].

2.4. Workpiece preparation and selected beam shapes

A schematic diagram of the welding cases is shown in Fig. 3. The workpiece sheet metal plates were steel S355MC, with dimensions

Table 1
Geometrical characteristics of the beam shapes.

Beam shape	Rx, mm	Ry, mm	Rx/Ry	BPP (mm·mrad)
C	0.40	0.40	1.00	8.690
TE	0.55	0.80	0.70	24.282

300 mm × 40 mm × 2 mm. The edges of the plates were grinded in segments so that the joint gap width was varying in those segments. Before linear welding, the plates were tack welded in 4 points (circular grey spots in Fig. 3).

Two distinct types of beam shapes were investigated: (i) circular with Gaussian intensity distribution; (ii) elliptical with Gaussian intensity distribution and major axis perpendicular to the welding travel direction. Such beam shapes are denoted by C (Gaussian Circular) and TE (Gaussian Transverse Elliptical). The corresponding beam shapes acquired by a PRIMES focus monitor mod. FM beam profiler in the focal planes is shown in Fig. 4, while in Table 1 the radii Rx and Ry of the LB focal spot along x and y directions, extracted by the beam shapes of Fig. 4, are reported.

2.4. Joint gap width and weld pool length measurements

The Joint gap width was measured in the acquired images at a small distance forward the weld pool. The position of the center point of this width extension was then translated backward to the point of the keyhole i.e., the LB center point in the subsequent and corresponding image to relate the weld pool top surface geometry to this measured gap width. The joint gap width estimation assumes that the gap remains constant between the point of measurement and the point of the LB as it passes the measuring point. The gap width expands in the x-direction perpendicular to the welding travel y-direction and was measured as w_c in the image coordinate system, and then translated to the world coordinate system $w_w = w_c * u$, where $u$is the resolution of the imaging system. The subsequent and corresponding image frame was found to measure the weld pool free surface geometry. The frame number was $N = \frac{(y-y_0)\times u}{v} \times f + N_0$, where v was the welding travel speed, N_0 was the frame number from which the gap width was measured, y_0 was the offset measured from the captured image frame where the laser was switched on. The center of the laser spot was fixed at y_0 in the image coordinate system.

As a following step, Canny edge detection was applied to get the weld pool surface contour from the selected N^{th} image. The solid-liquid boundary at the melt pools back side was identified by the difference in

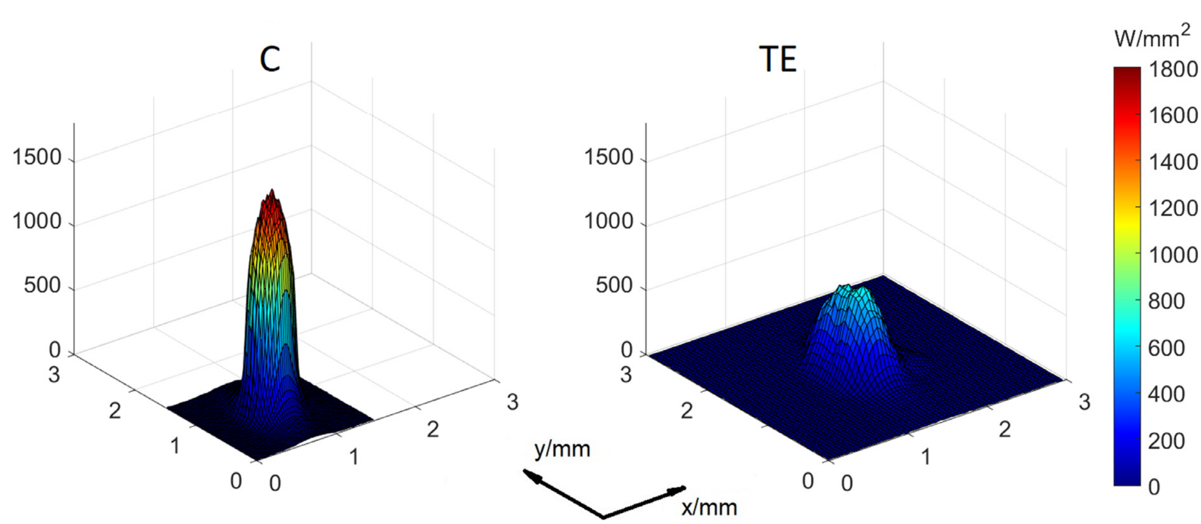

Fig.4. Beam shapes used during welding.

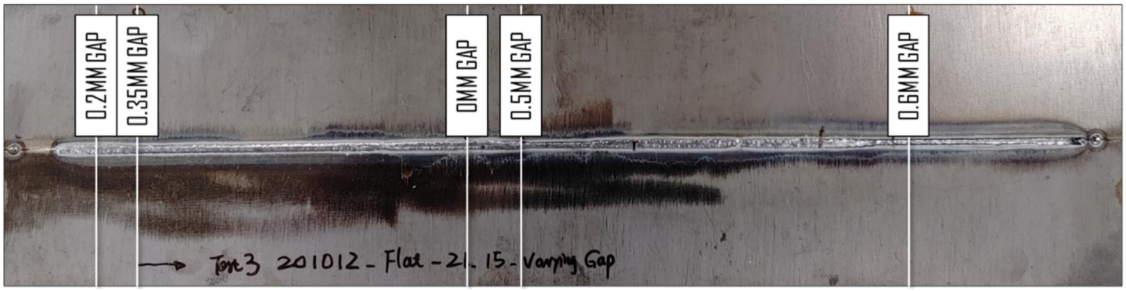

Fig. 5. Cross section positions at the corresponding gap width used in the metallographic analysis.

the textures of solidified material and the liquid metal. The melt pool front was identified by the reflection from the edges. The information and Canny edge detection results were combined to extract the melt pool boundary. The weld pool front and rearmost points along the welding direction were then identified on the solid liquid boundary contour edge. The length of the weld pool L_c in the image coordinate system was the distance between these two points and length in world coordinate was $L_w = L_c * u$.

To study the impact of the different beam shapes the weld pool length was measured at positions with a gap width of 0.0-mm, 0.2-mm, 0.35-mm, 0.5-mm, and 0.6-mm. For each of these cases the weld pool length was measured at two distinct positions with the same gap width along the joint and the two measurements were averaged.

2.5. Metallographic samples preparation after welding and measurement procedure

Plates welded by the C and TE beam shapes were analyzed by means of metallographic investigations. Two replications of each condition were used in the analysis. From each weld seam, five cross sections (as shown in Fig. 5) were extracted at locations corresponding to five different gap widths (0.0-mm, 0.2-mm, 0.35-mm, 0.5-mm, and 0.6-mm). Subsequently, each section was properly prepared (both by grinding and polishing) and then chemically etched with Nital (100 ml Ethanol 99% and 10 ml Nitric Acid 69%) for 15 s.

The cross sections were analyzed by means of a light microscope (Eclipse MA200 Nikon) and the Java-based software “ImageJ”. This software proved to be extremely useful to quantify in a robust way the different geometric regions of interest characterized by distinct microstructures, such as the Base Material (BM), the Heat Affected Zone (HAZ) and the Fused Zone (FZ). A scheme of the different investigated areas is reported in Fig. 6.

To evaluate the effect of both the gap and the beam shape, the following variables were examined and discussed in the following section: (i) the extension of the fused zone (FZ), (ii) the height of the FZ; (iii) the width of the FZ, and (iv) the extension of the HAZ.

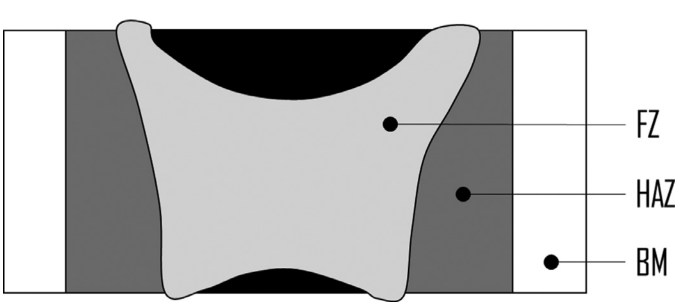

Fig. 6. Scheme of the different regions evaluated: *base metal* (BM), *fused zone* (FZ) and *heat affected zone* (HAZ).

3. Results and discussion

This section presents an investigation of the impact of the two investigated beam shapes (C and TE) at different gap widths. It is focused on the analysis of the weld pool top surface length and of the geometry of both the FZ and the HAZ.

3.1. Weld pool free surface visualization and measurements

Fig. 7 shows top view images of the weld pool resulting from the adoption of the two beam shapes at different joint gap widths.

The qualitative analysis of the images allows to notice that at small gaps (<0.35-mm) contours dimensions of the weld pool are significantly different due to the different type of beam shape. The weld pool determined by the C beam is much more elongated and tapered compared to the weld pool produced by the TE beam, which appears wider and shorter. This determines a welding condition, especially when the gap increases, which is much more unstable in the case of C beam. This is particularly evident when the 0.6-mm gap is considered, probably due to the large portion of the C beam passing through the gap, thus not sufficiently contributing to the melt of the edges. The keyhole is instable and partially collapsed and the weld pool very narrow and short. In the case of TE beam with the same gap of 0.6-mm, the welding is only slightly disturbed by the gap with a keyhole that appears still stable and with sufficient fusion of the edges. The small dark areas within the weld pool during elliptical beam welding was caused by image contrast enhancement. In the original image, these areas were greyed out. Besides, it was observed in the process top-view videos, that the regions moved from frame to frame, which indicates that they are probably oxides. Anyway, no pores could be detected from the analysis of the cross-sections, thus supporting the proposed interpretation of the black spots.

Quantitative results obtained by the image analysis procedure described in Section 2.4 are shown in Fig. 8, in which the length of the weld pool measured at different positions along the welding line are reported for both the investigated beam shapes.

In the case of the C beam, the length of the weld pool decreases from 7.3 mm to 5 mm as the width of the gap increases from 0 to 0.6 mm. Here, the most evident decrease in the weld pool length occurs when the gap becomes very large (0.6 mm) revealing that in such a case the gap is too wide to give the C beam the possibility to result in a stable weld pool. In the case of the TE beam, it is worth noticing that at small gaps the weld pool length is shorter than in the case of the C beam but also constant for all gap values, thus indicating a stable welding. In fact, even for the largest gap (0.6 mm) the length of the weld pool remains unchanged and significantly larger than the C beam. The possible reason is that the beam radius Ry (transverse to the gap) is larger than the maximal investigated gap width. This resulted in no significant change in material melting when the gap width was increased.

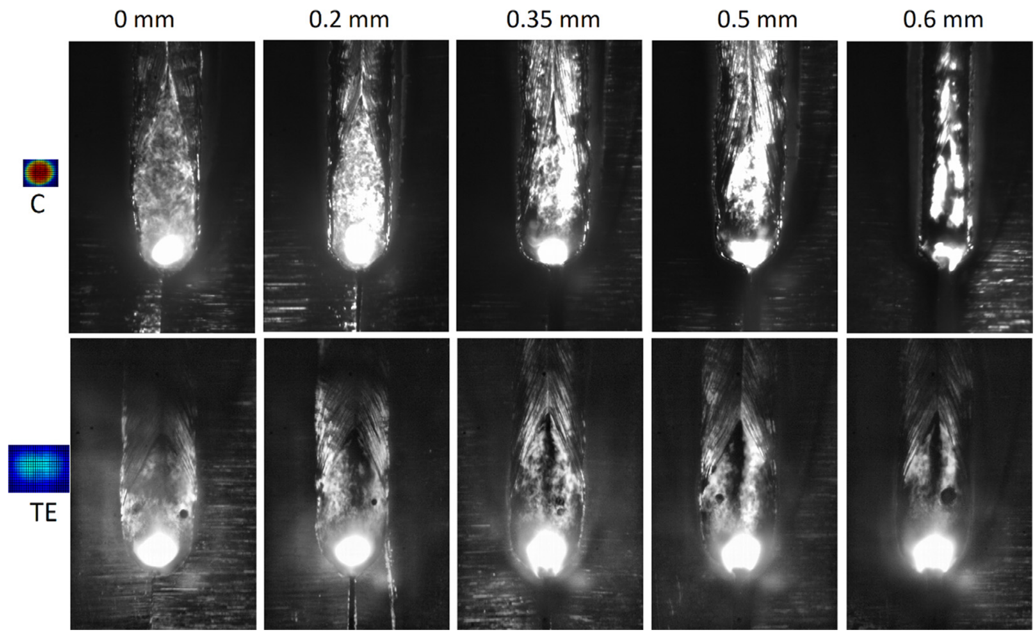

Fig. 7. Top view images of the weld pool with the beam shapes C and TE at different joint gap widths.

3.2. Metallographic analyses

Fig. 9 shows images of cross-sections of the weld seams obtained using the beam shapes (C and TE) at each of the investigated joint gap widths.

The analysis of the micrographs reveals that, when increasing the gap width, the TE beam results in a very regular weld seam shape.

To perform the analysis more quantitatively, the extensions of the different regions (FZ, HAZ) which characterize the weld seam were evaluated using the ImageJ software as a function of the gap width. Fig. 10 shows the FZ area versus the gap width.

It can be noticed that both beam shapes result in the same trend of the FZ, characterized by a maximum at a gap width of 0.2-mm. The reason why the FZ is larger is the presence of a gap, that even if small, improves the coupling of the laser radiation into the joint. Indeed, laser power absorption is improved when, thanks to the presence of a small gap, the beam penetrates deeper through multiple reflections. As the gap gets wider, the fraction of the beam that passes throughout the gap without being absorbed increases and results in a reduction of the FZ volume, thus showing up as a decreasing trend above the gap of 0.2 mm.

However, the two datasets also present evident differences. It can be noted that the TE beam is characterized by a smoother variation of the FZ according to the gap width than the C beam (in the case of the TE beam the extension of FZ ranges from a minimum of 3.5 mm^2 to a maximum of 4.3 mm^2, with a maximum variation of 16.9%). This is a clear indication that the TE beam allows a better coupling between the LB and the material, even in the case of the largest gap, due to an improvement of the heat transfer to the metal. Differently, when adopting the C beam, a much wider fluctuation of the FZ area is produced (beam the extension of FZ ranges between 2.9 mm^2 and 4.8 mm^2, with a maximum variation of 39.5%).

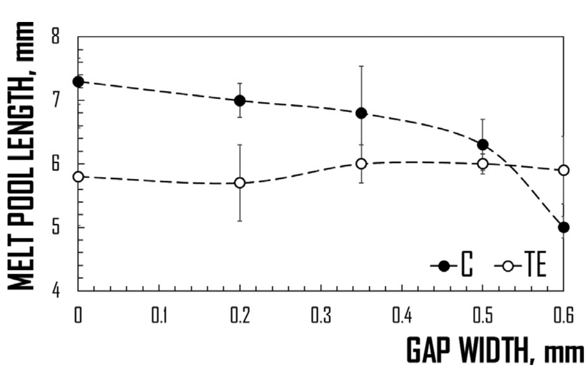

Fig. 8. Longitudinal length of the weld pool measured in top view images.

The height and the width of the FZ (in the cross section) were also evaluated and presented in Fig. 11 and Fig. 12, respectively. From a methodological point of view, the height values plotted in Fig. 11 are the average of three different measurements performed on each micrograph, taking the heights, respectively, at the joint central axis and at about 150 µm to the right and left sides.

As it can be seen from Fig. 11, irrespective of the beam shape, the joint height decreases with the widening of the gap. In fact, as the gap widens, the molten metal cannot fill the space between the two joint edges, so the FZ height decreases. However, the TE beam shape results in an improved consistency of the height of the FZ with the gap variation. More in detail, the height of FZ for the C beam varies between a maximum of about 2.0 mm to a minimum of about 1.4 mm for a gap of 0.2 mm and 0.5 mm, respectively (total reduction of about 33%). With the TE beam the height reduction is slightly lower (about 30%) indicating a higher resilience to keep the weld pool stable and bridge even large gaps. The difference is quite evident for a gap width of 0.5-mm where the TE beam produces a joint height 17% higher than the C beam shape.

Such a behavior is confirmed by the measurements of the widths of the FZ reported in Fig. 12. It is worth noticing that for all the investigated gap widths the TE beam produces joint widths always appreciably wider than the C beam. In addition, using the TE beam the width of the FZ has negligible changes when the gap increases. This aspect is particularly evident when the gap value considered is greater than 0.5 mm: in fact, in such a case the width of the FZ undergoes a sudden decrease when the C beam is used, while it is only slightly reduced when the TE beam is used, thus indicating the ability of the latter to mitigate and bridge gaps of similar dimensions.

In addition to the analysis of the FZ, the width of HAZ was also measured and the results reported in Fig. 13. The width of HAZ was not trivial to estimate since its contours are not clearly defined, and they are not uniform along the thickness direction. For this reason, the width of HAZ was estimated as follows (see the scheme proposed in the figure

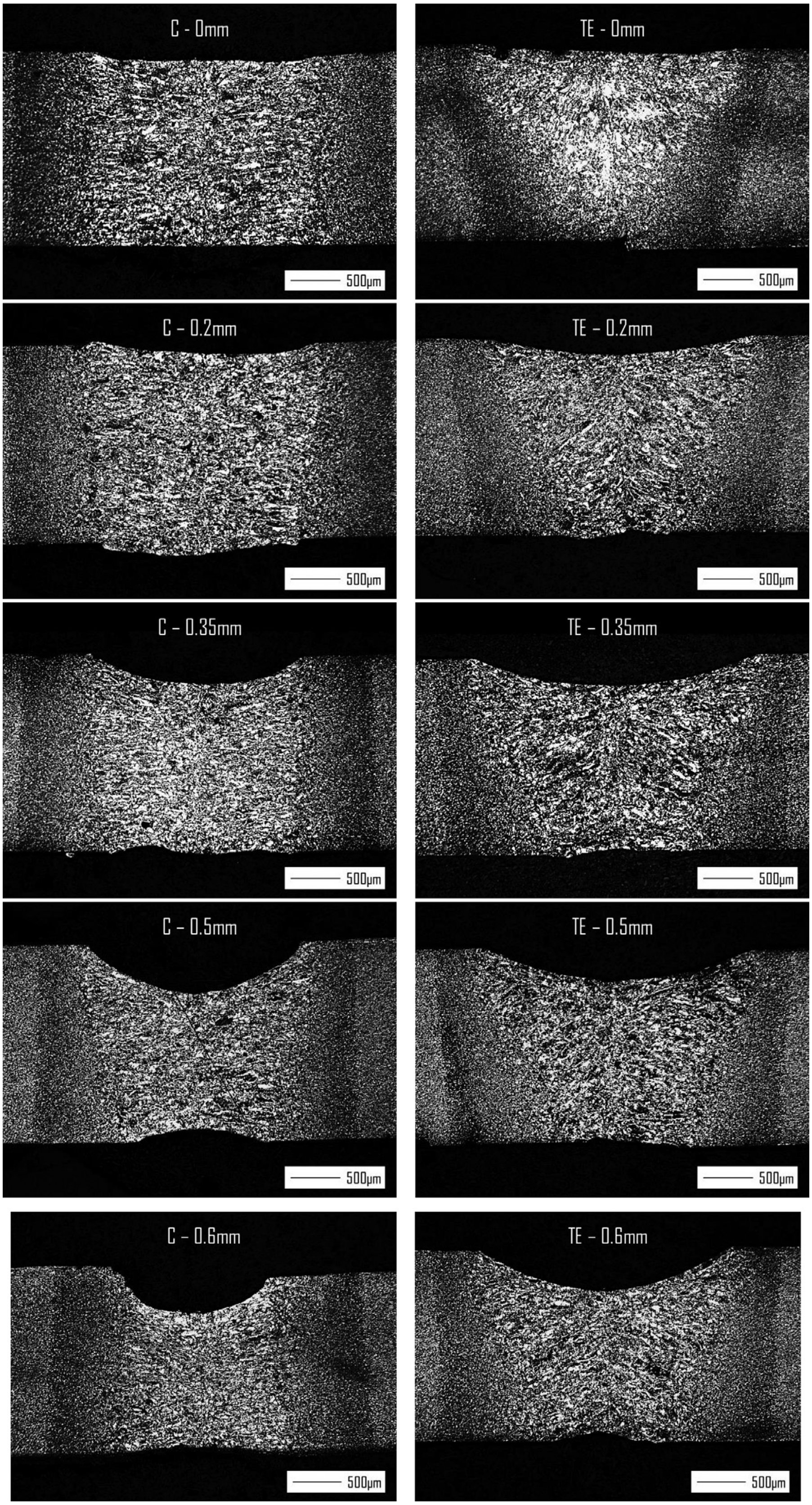

Fig. 9. Micrographs of the weld seams obtained by the beam shapes (C and TE) and at the different investigated joint gap widths.

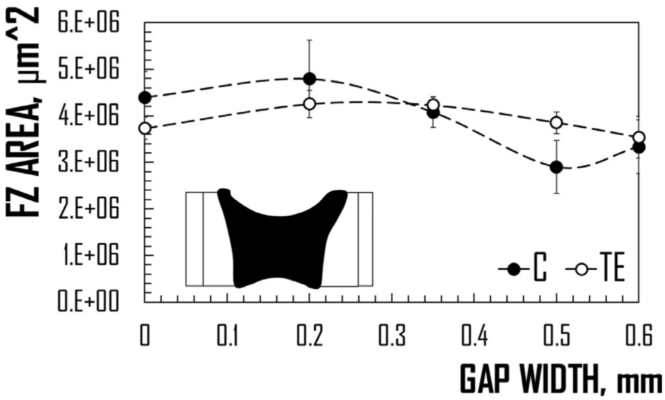

Fig. 10. The FZ cross section area at different joint gap widths using the two different beam shapes.

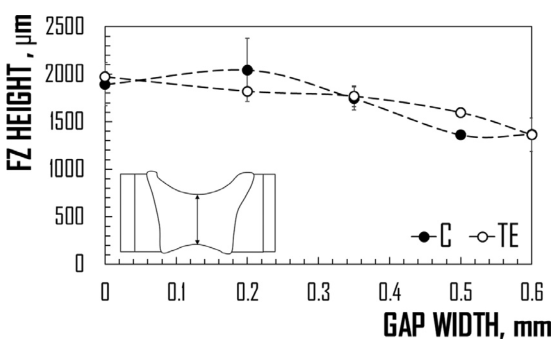

Fig. 11. FZ height as a function of the joint gap width for beam shapes C and TE.

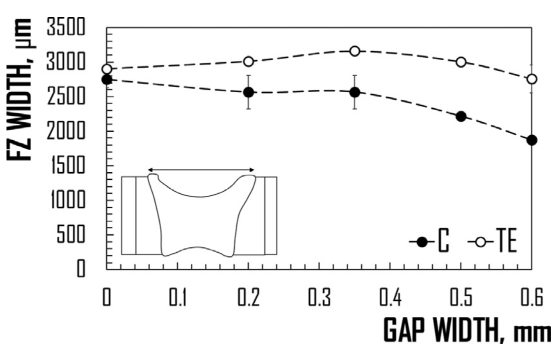

Fig. 12. FZ width as a function of the joint gap width for beam shapes C and TE.

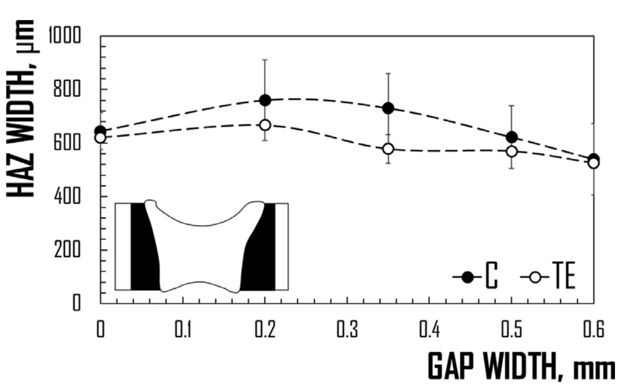

Fig. 13. Width of the HAZ as a function of the joint gap width at TE and C beam shapes.

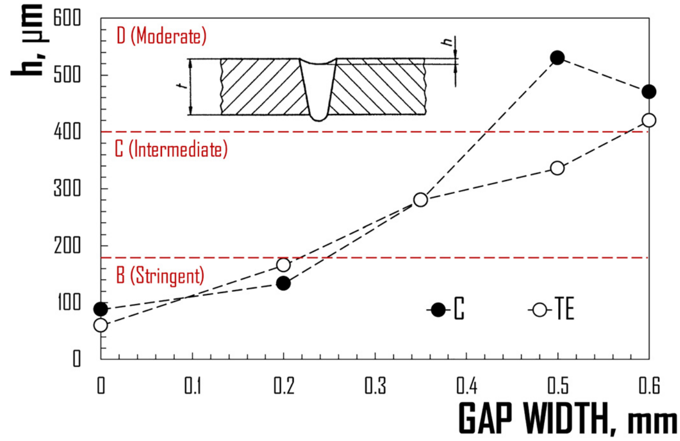

Fig. 14. Experimental h values according to the gap and the beam type.

inset): (i) the overall HAZ area was identified by the image processing software and measured; (ii) the area of HAZ was approximated to a rectangle whose height was the thickness of the workpiece (2 mm); (iii) the width of HAZ was calculated as the ratio between the area and the thickness of the workpiece. Data reported in Fig. 13 show a similar trend for the two beam shapes. The width of HAZ grows as far as the gap widens, until a maximum is reached (gap equal to 0.2 mm).

From this point, the width of the HAZ decreases reaching the smallest value at the widest gap (i.e., 0.6-mm). An important aspect is that the values obtained using the TE beam are always lower than those obtained using the C beam. In addition, the adoption of the TE beam guarantees less variations in the HAZ width as the gap varies (21% for the TE beam; 29% for the C beam).

Finally, according to the Standard ISO13919-1, it was possible to classify the quality of the welded zone through three different values such as B (stringent), C (intermediate) and D (moderate). This classification is based on the height (h) of the imperfection (as shown in the scheme in the graph in Fig. 14) related to the main size of the plate.

With reference to this, the values of h for all the investigated conditions have been calculated and reported in the previous graph. The two types of the beams (C and TE) have the same h values up to an intermediate gap (0.35 mm), after which the TE beam is much better than the C beam; in fact, the h value for the C beam increases more. According to this, it seems that while with C beam the transition from intermediate classification (C) to moderate classification (D) seems to occur for gaps of about 0.4 mm; using the TE beam, this transition covers larger gaps between 0.5 and 0.6 mm. Therefore, beam shaping on the fly following the gaps extension would allow, in principle, more relaxed tolerances in the preparations of the joints, still ensuring the manufacturing of butt joint with intermediate (C) weld quality.

The experimental results show that for smaller gaps, the C circular beam shape is more effective, while for larger gaps, elliptical beam shape is needed. To optimize this, on-line beam shaping could be used. One approach is to use a vision sensor to estimate the gap width and determine the beam profiles to apply during the process. The actuators of the deformable mirror will then be controlled to generate this beam shape, while the wavefront sensor continuously measures the aberrations. This procedure ensures that the desired beam shapes are attained and maintained, and the process would be efficient and robust.

4. Conclusions

An innovative approach has been proposed for the gap bridging in autogenous laser butt welding. In particular, the adoption of a deformable mirror allowed to efficiently change the laser beam shape from a Gaussian circular one to a Gaussian elliptical one having the major axis oriented transversely with respect to the welding direction (aspect ratio equal to 0.7).

Coupling quantitative information extracted by the top view images of the weld pool and the gap extension and data from micrographic analyses, it was possible to assess that when using the circular beam shape for gap widths wider than 0.35 mm (i.e., comparable with the size of the beam radius) the welding conditions became unstable, the weld pool was reduced and the keyhole collapsed, due to a significant portion of the laser beam passing through the gap without contributing to melt the material. On the contrary, the elliptical beam shape was able to make the welding conditions more stable, even up to gap widths of 0.5-mm.

Metallographic analyses allowed to quantify the dimensions of the main features of the weld seam (fused zone and heat affected zone), thus highlighting that:

- When using the elliptical beam, the quantity of the molten metal (in terms of height and width of the fused zone) remains almost unchanged when widening the gap, being also significantly higher than the correspondent parameters in the case of the circular beam.
- The elliptical beam shape is characterized by a smoother variation of the fused zone according to the gap width than the circular beam, thus indicating that the transverse elliptical beam allows a good coupling between the laser beam and the material, even in the case of the largest gap, due to an improvement of the heat transfer to the metal.
- The elliptical beam produces joint widths always appreciably wider than the circular beam.
- The elliptical beam produces heat affected zones characterised width values less than the ones produced by the circular beam, also guaranteeing less variations.

The proposed approach for the gap bridging allows, in principle, to produce many different beam shapes depending on the characteristics of the incoming beam, and the number, position and stroke of the actuators, thus making the laser beam optimal for any working condition, even with joints poorly or not prepared (large or not constant gaps).

Furthermore, such a technology would allow to vary the beam shape on-the-fly during welding, by implementing an intelligent algorithm which, based on the results of this work, will measure the gap width in real time and adapt the beam shape automatically through a closed-loop system.

Declaration of Competing Interest

The authors declare that they have no known competing financial interests or personal relationships that could have appeared to influence the work reported in this paper.

CRediT authorship contribution statement

Yongcui Mi: Investigation, Data curation, Writing – original draft. **Pasquale Guglielmi:** Data curation, Validation, Formal analysis, Writing – original draft. **Morgan Nilsen:** Data curation, Formal analysis, Writing – review & editing. **Fredrik Sikström:** Conceptualization, Methodology, Supervision, Writing – review & editing, Funding acquisition. **Gianfranco Palumbo:** Methodology, Supervision, Writing – review & editing. **Antonio Ancona:** Conceptualization, Investigation, Supervision, Writing – original draft.

Data availability

Data will be made available on request.

Acknowledgments

The authors gratefully acknowledge the Swedish Knowledge Foundation for granting the project AdOpt (20170315) and Dedicate (20210094), which supported the activities of this work. Special thanks go to Daniel Sthen from GKN Aerospace in Trollhättan (Sweden) and to Kjell Hurtig and Mats Högström from University West for their support during the experiments as well as to Dr. Stefano Bonora, from the CNR (Consiglio Nazionale delle Ricerche) Institute for Photonics and Nanotechnologies in Padova (Italy) for the valuable discussion and help with the deformable mirror system.

CRediT authorship contribution statement

All authors have read and agreed to the published version of the manuscript.

References

[1] Nilsen M, Sikström F, Christiansson A-K, Ancona A. Robust vision-based joint tracking for laser welding of curved closed-square-butt joints. Int J Adv Manuf Technol 2019;101:1967–78.
[2] Sun Z, Kuo M. Bridging the joint gap with wire feed laser welding. J Mater Process Technol 1999;87(1-3):213–22.
[3] Hansen KS, Olsen FO, Kristiansen M, Madsen O. Joining of multiple sheets in a butt-joint configuration using single pass laser welding with multiple spots. J Laser Appl 2015;27:032011.
[4] Volpp J. Multispot laser welding for increased gap bridgability. J Laser Appl 2022;34:042002.
[5] Kristiansen M, Kansen KS, Langbak A, Johansen SB, Krempin SB, Hornum MD. Single pass laser welding with multiple spots to join four sheets in a butt-joint configuration. Nordic laser materials processing conference NOLAMP16 Aalborg; 2017.
[6] Rasch M, Roider C, Kohl S, Strauss J, Maurer N, Nagulin KY, Schmidt M. Shaped laser beam profiles for heat conduction welding of aluminium-copper alloys. Opt Lasers Eng 2019;115:179–89.
[7] Volpp J, Vollertsen F. Impact of multi-focus beam shaping on the process stability. J Opt Laser Technol 2019;112:278–83.
[8] Meng Y, Jiang L, Cen L, Gao M. Improved mechanical properties of laser-arc hybrid welded Al-steel dissimilar butt-joint through beam oscillation. Sci Technol Weld Joining 2021;26:487–92.
[9] Chen X, Lei Z, Chen Y, Han Y, Jiang M, Tian Z, Bi J, Lin S, Jiang N. Effect of laser beam oscillation on laser welding–brazing of ti/al dissimilar metals. Materials 2019;12:4165.
[10] Kraetzsch M, Standfuss J, Klotzbach A, Kaspar J, Brenner B, Beyer E. Laser beam welding with high-frequency beam oscillation: welding of dissimilar materials with brilliant fiber lasers. International congress on applications of lasers & electro-optics; 2011.
[11] Thiel C, Hess A, Weber R, Graf T. Stabilization of laser welding processes by means of beam oscillation. Proc. of SPIE 2012;8433:84330V.
[12] Schaefer M, Kessler S, Scheible P, Graf T. Modulation of the laser power to prevent hot cracking during laser welding of tempered steel. J Laser Appl 2017;29:042008.
[13] A. Mahrle and E. Beyer, “Control of the energy deposition during laser beam welding by oscillation techniques”, in Proceedings of the 4th international WLT conference on lasers in manufacturing, 2007.
[14] Prieto C, Vaamonde E, Diego-Vallejo D, Jimenez J, Urbach B, Vidne Y, Shekel E. Dynamic laser beam shaping for laser aluminium welding in e-mobility application. Proc CIRP 2020;94:596–600.
[15] Dittrich D, Kessler B, Strohbach R, Jahn A. Laser beam welding of hot crack sensitive Al-alloys without filler wire by intensity controlled dynamic beam oscillation. Proc CIRP 2022;111:435–8.
[16] Möller M, Haug P, Scheible P, Buse C, Frischkorn C, Speker N. Spatially tailored laser energy distribution using innovative optics for gas-tight welding of casted and wrought aluminum alloys in e-mobility. J Laser Appl 2022;34:042015.
[17] S. Feuchtenbeiner, W. Dubitzky, T. Hesse, N. Speker, P. Haug, J. Seebach, J.-P. Hermani and D. Havrilla, “Beam shaping brightline weld: latest application results”, in Proceedings of the SPIE High power laser materials processing: applications, diagnostics, and systems VIII, 2019.
[18] Rinne JS, Nothdurft S, Hermsdorf J, Kaierle S, Overmeyer L. Advantages of adjustable intensity profiles for laser beam welding of steel copper dissimilar joints. Proc CIRP 2020;94:661–5.
[19] Mohammadpour M, Wang L, Kong F, Kovacevic R. Adjustable ring mode and single beam fiber lasers: a performance comparison. Manuf Lett 2020;25:50–5.
[20] E. Shekel, Y. Vidne and B. Urbach, “16kw single mode cw laser with dynamic beam for material processing”, in Fiber lasers XVII technology and systems, 2020.
[21] Wagner J, Heider A, Ramsayer R, Weber R, Faure F, Leis A, Armon N, Susid R, Tsiony O, Shekel E, Graf T. Influence of dynamic beam shaping on the geometry of the keyhole during laser beam welding. 12th CIRP conference on photonic technologies [LANE 2022], 4-8 September 2022 Fürth, Germany Procedia CIRP; 2022.
[22] Madec PY. Overview of deformable mirror technologies for adaptive optics and astronomy. Proc. SPIE 2012;8447(1):844705.
[23] Mrňa L, S M, Hola M. Deformable mirror for high power laser applications. Optics and measurement conference; 2014.
[24] Mi Y, Mahade S, Sikström F, Choquet I, Joshi S, Ancona A. Conduction mode laser welding with beam shaping using a deformable mirror. J Opt Laser Technol 2022;148:107718.
[25] Noori Rahim Abadi SMA, Mi Y, Sikström F, Ancona A, Choquet I. Effect of shaped laser beam profiles on melt flow dynamics in conduction mode welding. Int J Therm Sci 2021;166:106957.